AD-A160 359 EXPERIMENTAL RUNS WITH A LOW-ORDER MODEL OF A MOIST GENERAL CIRCULATION.. (U) MASSACHUSETTS INST OF TECH CAMBRIDGE CENTER FOR METEOROLOGY A.. E N LORENZ

UNCLASSIFIED 31 MAY 85 AFGL-TR-85-0118 F19628-83-K-0012 F/G 4/2 NL

1/1

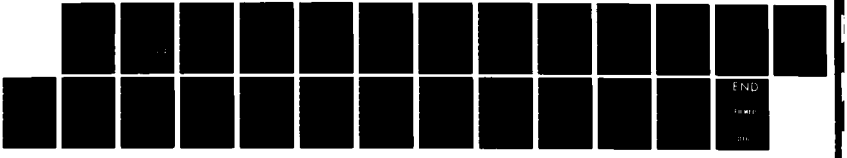

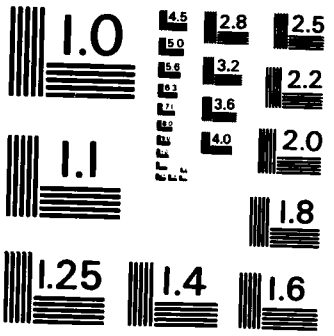

MICROCOPY RESOLUTION TEST CHART
NATIONAL BUREAU OF STANDARDS - 1963 - A

(12)

AFGL-TR-85-0118

EXPERIMENTAL RUNS WITH A LOW-ORDER MODEL OF A MOIST GENERAL CIRCULATION

Edward N. Lorenz

Center for Meteorology and Physical Oceanography
Department of Earth, Atmospheric, and Planetary Sciences
Massachusetts Institute of Technology
Cambridge, Masachusetts 02139

31 May 1985

Final Report
24 November 1982 - 31 March 1985

AIR FORCE GEOPHYSICS LABORATORY
AIR FORCE SYSTEMS COMMAND
UNITED STATES AIR FORCE
HANSCOM AFB, MASSACHUSETTS 01731

"This technical report has been reviewed and is approved for publication"

CHIEN-HSIUNG YANG
Contract Monitor

DONALD A. CHISHOLM, Chief
Atmospheric Prediction Branch

FOR THE COMMANDER

ROBERT A. McCLATCHEY, Director
Atmospheric Sciences Division

This report has been reviewed by the ESD Public Affairs Office (PA) and is releasable to the National Technical Information Service (NTIS).

Qualified requestors may obtain additional copies from the Defense Technical Information Center. All others should apply to the National Technical Information Service.

If your address has changed, or if you wish to be removed from the mailing list, or if the addressee is no longer employed by your organization, please notify AFGL/DAA, Hanscom AFB, MA 01731. This will assist us in maintaining a current mailing list.

Unclassified
SECURITY CLASSIFICATION OF THIS PAGE

AD-A160 357

REPORT DOCUMENTATION PAGE

1a. REPORT SECURITY CLASSIFICATION: Unclassified	1b. RESTRICTIVE MARKINGS:
2a. SECURITY CLASSIFICATION AUTHORITY:	3. DISTRIBUTION/AVAILABILITY OF REPORT: Approved for public release; distribution unlimited
2b. DECLASSIFICATION/DOWNGRADING SCHEDULE:	
4. PERFORMING ORGANIZATION REPORT NUMBER(S):	5. MONITORING ORGANIZATION REPORT NUMBER(S): AFGL-TR-85-0118
6a. NAME OF PERFORMING ORGANIZATION: Massachusetts Institute of Technology; 6b. OFFICE SYMBOL (If applicable):	7a. NAME OF MONITORING ORGANIZATION: Air Force Geophysics Laboratory (LYP)
6c. ADDRESS (City, State and ZIP Code): Ctr for Meteorology & Physical Oceanography, Dept of Earth, Atmospheric & Planetary Sciences, Cambridge, MA 02139	7b. ADDRESS (City, State and ZIP Code): Hanscom AFB, Massachusetts 01731
8a. NAME OF FUNDING/SPONSORING ORGANIZATION: Air Force Geophysics Laboratory; 8b. OFFICE SYMBOL (If applicable):	9. PROCUREMENT INSTRUMENT IDENTIFICATION NUMBER: F19628-83-K-0012 - Final Report
8c. ADDRESS (City, State and ZIP Code): Hanscom AFB, Massachusetts 01731	10. SOURCE OF FUNDING NOS.

PROGRAM ELEMENT NO.	PROJECT NO.	TASK NO.	WORK UNIT NO.
61102F	2310	G7	AD

11. TITLE (Include Security Classification): Experimental Runs With a Low-Order Model of a Moist General Circulation

12. PERSONAL AUTHOR(S): Edward N. Lorenz

13a. TYPE OF REPORT	13b. TIME COVERED	14. DATE OF REPORT (Yr., Mo., Day)	15. PAGE COUNT
Final	FROM 11/24/82 TO 3/31/85	1985 May 31	24

16. SUPPLEMENTARY NOTATION

17. COSATI CODES		
FIELD	GROUP	SUB. GR.

18. SUBJECT TERMS (Continue on reverse if necessary and identify by block number): Moist general circulation; Albedo; Low-order model; Cloud-feedback; Thermodynamic and radiative effects of water

19. ABSTRACT (Continue on reverse if necessary and identify by block number)

We have made some experimental runs with a very-low-order general-circulation model, which includes the thermodynamic and radiative effects of water vapor and liquid water in the atmosphere. We first made several runs lasting 20 years or longer, to determine suitable combinations of values of model parameters for use in subsequent experiments. Using one "suitable" combination, we made one 450-year run, and found that the globally averaged temperature underwent long-period fluctuations with a range of about two degrees, resembling real atmospheric "climatic" changes. In some final runs we suppressed the influence of cloudiness on the global albedo, and found that this modification eliminated the high sensitivity of the temperature to the planetary temperature and the very slow approach of the temperature to equilibrium, which characterized the ordinary runs.

20. DISTRIBUTION/AVAILABILITY OF ABSTRACT	21. ABSTRACT SECURITY CLASSIFICATION
UNCLASSIFIED/UNLIMITED ☐ SAME AS RPT ☒ DTIC USERS ☐	Unclassified

22a. NAME OF RESPONSIBLE INDIVIDUAL	22b. TELEPHONE NUMBER (Include Area Code)	22c. OFFICE SYMBOL
Chien-Hsiung Yang	617-861-3913	LYP

DD FORM 1473, 83 APR EDITION OF 1 JAN 73 IS OBSOLETE.

Unclassified
SECURITY CLASSIFICATION OF THIS PAGE

1. Introduction

During the past decade our group has been investigating the manner in which the presence of water in the atmosphere affects the large-scale atmospheric circulation. Our work has been performed under a number of consecutive contracts with the Air Force Geophysics Laboratory. Our more recent work has centered about the formulation of a low-order model in which water occupies a key postion. We have constructed the model so that separate properties of water may be suppressed, individually or in combination, and the resulting changes in the circulation may be ascertained.

The model is an extension of the familiar dry two-layer quasi-geostrophic beta-plane model, as originally formulated by Phillips (1951). Isobaric height (or stream function) and temperature at any reference level may be chosen as the basic prognostic dependent variables in the dry model. Velocity potential and individual pressure change appear as auxiliary variables, determined diagnostically from the height and temperature fields. To these we have appended total dew point and ocean-surface temperature as basic prognostic variables, to produce a moist model. Ordinary dew point, relative humidity, water-vapor mixing ratio, liquid water mixing ratio, and saturation mixing ratios at atmospheric and oceanic temperatures enter as additional diagnostically determined variables. For a reference level we have chosen the earth's surface (1000 mb).

The diabatic processes include viscous drag, sensible-heat transfer, evaporation and precipitation, and short-wave and long-wave radiation.

We have made the model "low-order" by expressing each basic-variable field as a double Fourier series, and then truncating each series to include only seven terms, just as we previously did in formulating a low-order dry model used to study vacillation (Lorenz, 1963). A complete description of the model appears in the final report of the most recently completed contract (F 19628-81-K-001), entitled "A low-order model of a moist general circulation: formulation and testing". A similar description, accompanied by some "synoptic maps" produced by the model, appears in the Journal of the Atmospheric Sciences (Lorenz, 1984), under the title "Formulation of a low-order model of a moist general circulation".

In that article we describe a set of three preliminary numerical runs made with the model, each lasting 500 days. In the initial run the chosen cross-latitude contrast in solar heating produces a zonal flow, which becomes unstable with respect to Rossby-wave perturbations upon acquiring sufficient strength; the perturbations subsequently grow to become fully developed waves. In the final state of the final run, which seems to be representative, the surface map contains a succession of cylones and anticyclones. The highest relative humidities occurred somewhat to the NNE of the cyclone centers, while the maximum rates of precipitation occur somewhat to the SE. The strongest evaporation occurs in the southern portions of the anticyclones.

On the negative side of the ledger, the cyclones and anticyclones are much weaker than typical systems in the real atmosphere. On occasions during the runs the model systems attain more realistic amplitudes. We concluded that the model behaved in a qualitatively

reasonable manner, and that, with possible adjustments in the numerical values of some of the parameters, it was ready for production runs.

Most of our computations, including those which formed the three preliminary runs, have been carried out with a relatively slow system. This report describes a limited number of runs which were performed on the Cray-1 computer at the National Center for Atmospheric Research. This system is about three orders of magnitude faster than the system which we have customarily used, and it will integrate the equations of our model for one year of simulated time in about 1.3 seconds.

In the sections which follow we first describe some experiments using various combinations of values of the model parameters, designed primarily to determine suitable combinations for use in subsequent experiments. We next describe a very long run performed with "suitable" parameter values, which produced fluctuations with strikingly long periods. Finally we present some comparison runs in which the influence of cloudiness on the earth's albedo has been suppressed.

2. Some adjustable model parameters

As we have already noted, the cyclones and anticyclones which develop in the preliminary runs with the model are much weaker than their real atmospheric counterparts. In our detailed write-up we mentioned that this discrepancy might have resulted from an excessively high static stability, a weak cross-latitude temperature contrast, or some other unidentified cause. The experiments to be described in this section represent a first attempt to account for the discrepancy, and to eliminate it by choosing new parameter values, i.e., to tune the model.

The model has a preassigned constant lapse rate of temperature, which is introduced by letting the temperature in each vertical column vary as p^{λ}, where p is pressure. When $\lambda = \kappa = 2/7$, the lapse rate is dry adiabatic. In the preliminary runs we set $\lambda = 0.175$, or about 0.61 times the dry-adiabatic value. We noted, incidentally, that the use of a fixed static stability was one of the main shortcomings of the model, which we hoped eventually to remove, at least to the extent of letting λ vary with time.

The model atmosphere extends horizontally over an infinite channel, bounded on the south and north by frictionless walls at $y = 0$ and $y = \pi$. The basic variables, but not the auxiliary variables, assume the form

$$X = \sum_{n=0}^{6} X_n \Phi_n \quad , \qquad (1)$$

where X may be the stream function ψ, temperature T, total dew point W, or ocean-surface temperature S, and

$$\left.\begin{aligned} \Phi_0 &= 1 \\ \Phi_1 &= 2 \sin y \cos 2x \\ \Phi_2 &= 2 \sin y \sin 2x \\ \Phi_3 &= \sqrt{2} \cos y \\ \Phi_4 &= 2 \sin 2y \cos 2x \\ \Phi_5 &= 2 \sin 2y \sin 2x \\ \Phi_6 &= \sqrt{2} \cos 2y \end{aligned}\right\} \qquad (2)$$

The zonally symmetric flow is given by the terms in eq.(1) with n = 0, 3, 6, while the remaining terms represent a chain of large-scale

Rossby waves. A superposition of waves on a suitable zonal flow produces cyclones and anticyclones. The solar heating is expressed in terms of a "planetary" temperature field T*, whose value at any location is the temperature which a black body covering the entire sky would have to be equivalent to the sun. In the preliminary runs we chose

$$T^* = T_0^* \Phi_0 + T_3^* \Phi_3, \qquad (3)$$

so that T_3^* measured the heating contrast, and we let $T_0^* = 273.0$ and $T_3^* = .0$ (we quote all values of T, W, and S in degrees Kelvin).

A feature of the model's behavior which became apparent in the preliminary runs, and must be recognized if the tuning process is to succeed, is the high sensitivity of the temperature T to the planetary temperature T*, and particularly of the globally averaged surface temperature T_0 to the globally averaged planetary temperature T_0^*. This appears to result from a cloud-albedo feedback process. Increased solar heating not only heats the air, but also tends to lower the relative humidity and the accompanying cloudiness (although the specific humidity increases), thus allowing more solar energy to reach the earth, and warming the atmosphere still more. An accompanying feature is the very slow rate at which T_0 approaches its ultimate value from a prechosen initial state. It is as though the temperature were attempting to reach an equilibrium, and, having nearly reached it, discovered that the rules had been changed and that it must approach another equilibrium.

One property of the real atmosphere-ocean system which, if present in the model, would make the approach to equilibrium very slow is the high ratio R of the heat capacity of the upper layer of the ocean to that

of the atmosphere. For an oceanic mixed layer 70 meters deep, interacting with the atmosphere, R would be about 30. In our preliminary runs, in order to reduce the required computation time, we let R = 1, so that the ocean might more properly have been considered to be wet land. Despite the small value of R, the approach to equilibrium was slow.

The runs to be described make use of various values of λ, T_0^*, T_3^*, and R. All other adjustable model parameters retain the values used in the preliminary runs.

3. Tuning the model

Our first run, which we shall call Run 1, was performed to determine whether the final preliminary run had indeed reached equilibrium, and it therefore used the same parameter values. Not knowing how much time might really be needed to attain equilibrium, we let the model run for 25 years, starting with a small perturbation ($\psi_1 = 0$, $T_1 = W_1 = S_1 = 1.0$) superposed on the zonally symmetric (but not steady) fields $\psi = 0$, $T = W = S = T^*$. Fig. 1 shows instantaneous values of T_0 at three-month intervals. After a brief initial drop, T_0 increases continually, although somewhat erratically, attaining a peak value of 280.1 in 16.5 years. Thereafter it drops slightly, eventually undergoing fluctuations, with a range of about 0.3, about a mean of 279.7.

The final preliminary run and the new run are entirely consistent, except that T_0, W_0, and S_0 are about one degree too low in the former. The cross-latitude temperature contrast T_3 is about twice T_3^*, as a result of the sensitivity of T to T*, while the Rossby waves are uniformly weak.

We next performed two 25-year runs, again with $\lambda = 0.175$ and $R = 1.0$, but with $T_3^* = 15.0$, and with $T_0^* = 273.0$ in Run 2 and 270.0 in Run 3. Both runs finally reached quasi-equilibrium, but with T_0 fluctuating around 284.9 in the former run and 271.1 in the latter. Thus the two values of T_0 differed by more than 4 times the corresponding difference in T_0^*. Moreover, increasing T_3^* from 5.0 to 15.0 increased T_0 by more than five degrees, even though T_0^* remained fixed, but T_3 increased only slightly, from 10.7 to 13.1. Evidently these values of T_3 are comparable to the minimum value needed for baroclinic instability. The waves approximately doubled in amplitude, but were still rather weak. In all cases the waves in the W-field were stronger than those in the T-field, while those in the S-field were barely detectable.

The new runs did not acquire steady states, since the Rossby waves continued to progress eastward. Moreover, even the zonally symmetric components T_0, T_3, and T_6 continued to fluctuate. The nature of these fluctuations is revealed by Fig. 2, which shows instantaneous values of T_0 in Run 2, at 3-hour intervals for 25 days. Accompanying these values are horizontal line segments indicating the times when T_1 and T_4, the cosine phases of the two wave modes in the T field, are positive. There are periodic oscillations with a range of about 0.4 K and a period of about 11.2 days. This is evidently the time required for the second wave mode ($T_4\ \Phi_4 + T_5\ \Phi_5$), traveling at about 20 m s^{-1}, to move one wave length (5750 km) farther than the first wave mode($T_1\ \Phi_1 + T_2\ \Phi_2$), traveling at about 14 m s^{-1}. These modes interact with T_3 through an advective (quadratic) nonlinearily, while T_3 affects T_0 through a higher-degree nonlinearity. Thus vacillation is occurring.

Superposed on this oscillation is a weaker fluctuation with a period of about 1.1 days, which appears to be the time required for the second wave mode to travel 1/3 wave length. This time is significant because, in integrating the equations, we transform back and forth between Fourier modes and grid points during each time step. The west-east spacing of the grid points is three per wave length. We evaluate the high-degree nonlinear terms which enter the radiation and moist thermodynamic formulas at grid points; the total effect of these terms on T_0 differs according to whether a wave trough (or ridge) is located close to a grid point or almost midway between grid points.

We could virtually eliminate this effect by using a denser network of grid points, but this would conflict with our aim of keeping the model as small as possible. We prefer to keep the model as it is, and regard it as possessing weak periodic topography with a period of one grid interval. The effect of such topography would be to produce oscillations like the shorter-period ones in Fig. 2.

Similar doubly periodic oscillations occur in Runs 1 and 3. The apparent 15-month periodicity occurring during the last 6 years in Fig. 1 is actually a short-period oscillation, which has been aliased by being sampled only once every three months. The two short periods in Fig. 2 appear incommensurable, but there is no evidence of aperiodicity.

For Run 4 we have increased λ to 0.2, while letting $T_0 = 273.0$, $T_j = 10.0$, and $R = 1.0$. In Fig. 3 the vertical line segments show the total range of T_0 during each three-month interval. Again T_0 appears to be seeking an equilibrium, but the fluctuations are more pronounced than those appearing in Fig. 1. Moreover, they are not merely aliased

On the basis of Runs 1-6 we have decided that the values $\lambda = 0.2$, $T_0^* = 273.0$, $T_3^* = 10.0$, and $R = 10.0$ are suitable for further runs. It appears unlikely that such runs will ever settle down to steady behavior, so that a considerable variety of initial states should be compatible with the climate. These should include any state in the later years of Run 6, but suitable states also appear to be reached after a few months from the simple initial state consisting of a small perturbation, $T_1 = W_1 = S_1 = 1.0$, superposed on the zonally symmetric state where $\psi_0 = 0$, $T_0 = 287.0$, $W_0 = 284.5$, $S_0 = 286.5$, $\psi_3 = 0$, $T_3 = 6.0$, $W_3 = 4.5$, $S_3 = 5.5$, and $\psi_6 = T_6 = W_6 = S_6 = 0$.

4. Low-frequency fluctuations

The later years of Run 4 reveal considerable irregular variability, with peak values of T_0 occurring at 1- to 2-year intervals. In Run 6, where R has been increased to 10.0, peaks show some sign of occurring at 5- to 10-year intervals, and a general downward trend is evident. To determine whether the low-frequency fluctuations and the downward trend continue, we have extended Run 6 for 370 additional years; the entire 450 years constitute Run 7.

Fig. 6 shows the successive annual averages of T_0 for the final 400 years of Run 7, which begin shortly after the peak value in Fig. 5 has been atttained. The downward trend soon ceases, and there appear to be irregular variations on all time scales. The total range of T_0 exceeds two degrees. Changes from one year to the next seldom exceed 0.4, while increases or decreases of 1.0 or more generally require 10 years or longer. Ten-year averages vary nearly as much as annual averages, while

short-period oscillations. Such oscillations, with a range of about 0.5 K, could possibly account for the lengths of the segments, but the presence of completely non-overlapping segments, some less than a year apart, shows that longer-period fluctuations are also present. Similarly drawn segments for the final years of Run 1 would show no variability at all.

Meanwhile T_3 fluctuates about a mean value of about 5.6; this value, about half of that in Runs 1-3, is apparently large enough to produce baroclinic instability with the steeper lapse rate ($\lambda = 0.2$). The waves are now about 4 times as strong as in Run 1, and have entered the atmospheric range.

To observe the effect of using a more realistic oceanic heat capacity, we have performed Run 5, which is like Run 4 except that $R = 25.0$. The result is indicated by the dots in Fig. 4, which, as in Fig. 1, show instantaneous values of T_0. After 15 years, T_0 seems no closer to equilibrium than it was after 2 years in Run 4. Determining the final equilibrium could be a laborious task.

As a compromise we have performed Run 6, with $R = 10.0$ and with the other parameters unchanged from Run 4, and have used the final conditions of Run 4 as initial conditions. In Fig. 5 the vertical segments indicate the total range of T_0 in each of 80 successive years. Within each year the annual range is comparable to 1.0. The annual mean increases, with one lapse, for almost 20 years; thereafter it remains reasonably steady for another 20 years. During the later years there is a general downward trend, and T_0 loses a full degree. The annual mean values of W_0 behave similarly, and in fact almost exactly fit the linear relation

$T_0 - 287.2 = 1.2(W_0 - 284.5)$.

even 50-year averages are insufficient for estimating true climatic means; during years 100-150 the average T_0 is 287.1, while during years 200-250 it is 287.8. Apparently the variations of T_0 are dominated by very low frequencies.

A one-degree change in a local temperature is not a very striking event. The significance of the changes shown in Fig. 6 is that they are changes in the globally and annually averaged temperature, and that variations of the global annual average temperature of the real atmosphere seem to be of comparable magnitude, occurring on comparable time scales (cf. Pan and Oort, 1983). In all likelihood a warming or cooling of the real atmosphere, proceeding more or less continually for 10 or 20 years, and totaling one degree, would be interpreted by many observers as a climatic change, and attempts might be made to determine a cause.

In the model there is no special cause for these changes; they simply represent the model's natural variability. There are no changes whatever in the solar output, nor in any other conditions external to the atmosphere and ocean. While a model as simple as this one can yield only limited information about the real atmosphere, it at least shows that changes having the magnitude and time scale of those encountered in Run 7 do not necessarily demand external causes.

5. Comparison runs

One of our principal motives for constructing the low-order moist model was our wish to investigate the influence of water on the

circulation of the atmosphere, by comparing ordinary runs with special runs in which the influence of water is treated differently. Here we shall compare the runs described in the previous section with runs in which the influence of clouds on the earth's albedo has been suppressed. In the new runs we have given the albedo the constant value of 0.297; this is the value which it will assume in an ordinary run when T = 285.0.

In the first three new runs we have let T_0^* = 270.0, 273.0, and 276.0, while, as in Run 4, λ = 0.2, T_3^* = 10.0, and R = 1.0. In each run quasi-equilibrium is attained in less than two years. The equilibrium values of T_0 are about 281.0, 284.1, and 287.9, while the values of T_3^*, and the intensities of the cyclones and anticyclones, are comparable to those in Run 4. The high sensitivity of T_0 to T_0^* is no longer present. Clearly this sensitivity and the slow approach to equilibrium in the ordinary runs are associated in some way with the variable albedo.

In the next three new runs we have let T_3^* = 4.0, 8.0, and 12.0, while, again as in Run 4, λ = 0.2, T_0^* = 273.0, and R = 1.0. The first new run settles down after slightly more than a year to steady zonally symmetric equilibrium, with T_0 = 283.0 and T_3 = 4.9; evidently this value of T_3 is insufficient for baroclinic instability. In the other new runs the waves persist, becoming somewhat weaker than those in Run 4 in the run where T_3^* = 8.0, and acquiring comparable intensity when T_3^* = 12.0. The respective values about which T_3 continues to fluctuate are about 5.2 and 5.5, which evidently exceed the baroclinic-instability criterion. It thus appears that, in the present model, a cloud-albedo process can enhance the ability of a weak cross-latitude heating contrast to produce baroclinic instability.

In our final new run we have increased R to 10.0, while again letting $\lambda = 0.2$, $T_0 = 273.0$, and $T_3^* = 10.0$. With this high oceanic heat capacity nearly 10 years are needed for T_0 to attain quasi-equilibrium, but the approach is still considerably more rapid than in Run 4, where the heat capacity is low (R = 1.0) but the cloud-albedo feedback is present.

Additional alterations of physical processes which might be made in comparison runs are almost limitless. The examples which we have described are sufficient to show that simple changes can have pronounced effects.

6. Concluding remarks

Provided that one possesses a numerical model to work with, one can test the importance of a physical process which is present in the model by determining the typical behavior of the model, and subsequently inactivating the physical process in question and observing how the behavior of the model has been altered. We have demonstrated that this technique can be used even with a very-low-order model. Our model was designed to deal with an atmosphere which possesses an important constituent which occurs with variable concentration and in more than one phase. In our applications we have identified the atmosphere with the earth's atmosphere, and the constituent with water.

We have presented one example indicating that the equilibrium state about which the model atmosphere will fluctuate, and the rate at which it will approach this equilibrium from an unbalanced state, are strongly

influenced by a cloud-albedo feedback process. This result may not hold up too well in the real world, since it appears that the model may exaggerate either the influence of clouds on the albedo or the extent to which cloudiness varies. Nevertheless, we have shown that the model may be tuned to fit the earth's atmosphere more closely. Additional tuning, perhaps by changing the value of the parameter representing the "half life" of liquid water, i.e., the time during which liquid water tends to persist as clouds before falling out as rain, could bring about a still better fit. Also there are relevant physical processes which for simplicity we have omitted, but which could easily be introduced.

Beyond these considerations, we have devoted considerable attention to one of the more interesting and unexpected model phenomena to be discovered, namely, the pronounced long-term fluctuations of the globally averaged temperature, which resemble climatic changes. A natural conclusion is that the model might find use as a climate model. It would not be too difficult to change to spherical geometry, and introduce such features as seasonal variations in the solar forcing, and the presence of polar ice, which a climate model ought to possess. The great advantage of our model is its speed; with a large computer, runs of 1,000 or even 10,000 years are entirely feasible. We venture a guess that the model, with suitable additions, could prove capable of creating an ice age from an interglacial initial state, or vice versa, even though the numerical integration must proceed in 1.5-hour time steps.

References

Lorenz, E. N., 1963: The mechanics of vacillation. J. Atmos. Sci., 20, 448-464.

Lorenz, E. N., 1984: Formulation of a low-order model of a moist general circulation. J. Atmos. Sci., 41, 1933-1945.

Pan, Y. H. and A. H. Oort, 1983: Global climate variations connected with sea surface temperature anomalies in the eastern equatorial Pacific Ocean for the 1958-73 period. Mon. Wea. Rev., 111, 1244-1258.

Phillips, N. A., 1951: A simple three-dimensional model for the study of large-scale extratropical flow patterns. J. Meteor., 8, 381-394.

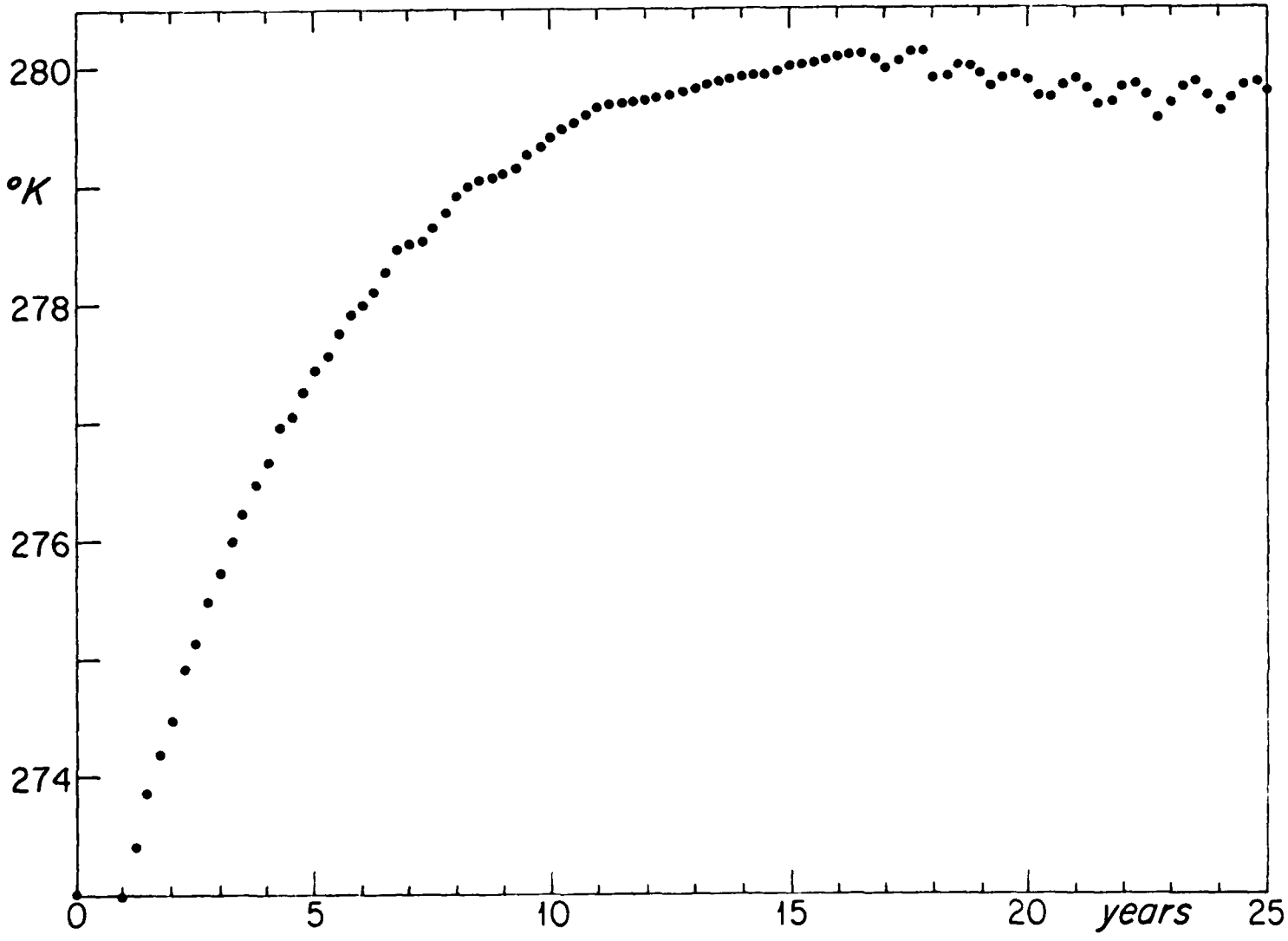

Fig. 1. Instantaneous values of T_3 at 3-month intervals in Run 1, where $\lambda = 0.175$, $T_0 = 273.0$, $T_3^* = 5.0$, and $R = 1.0$.

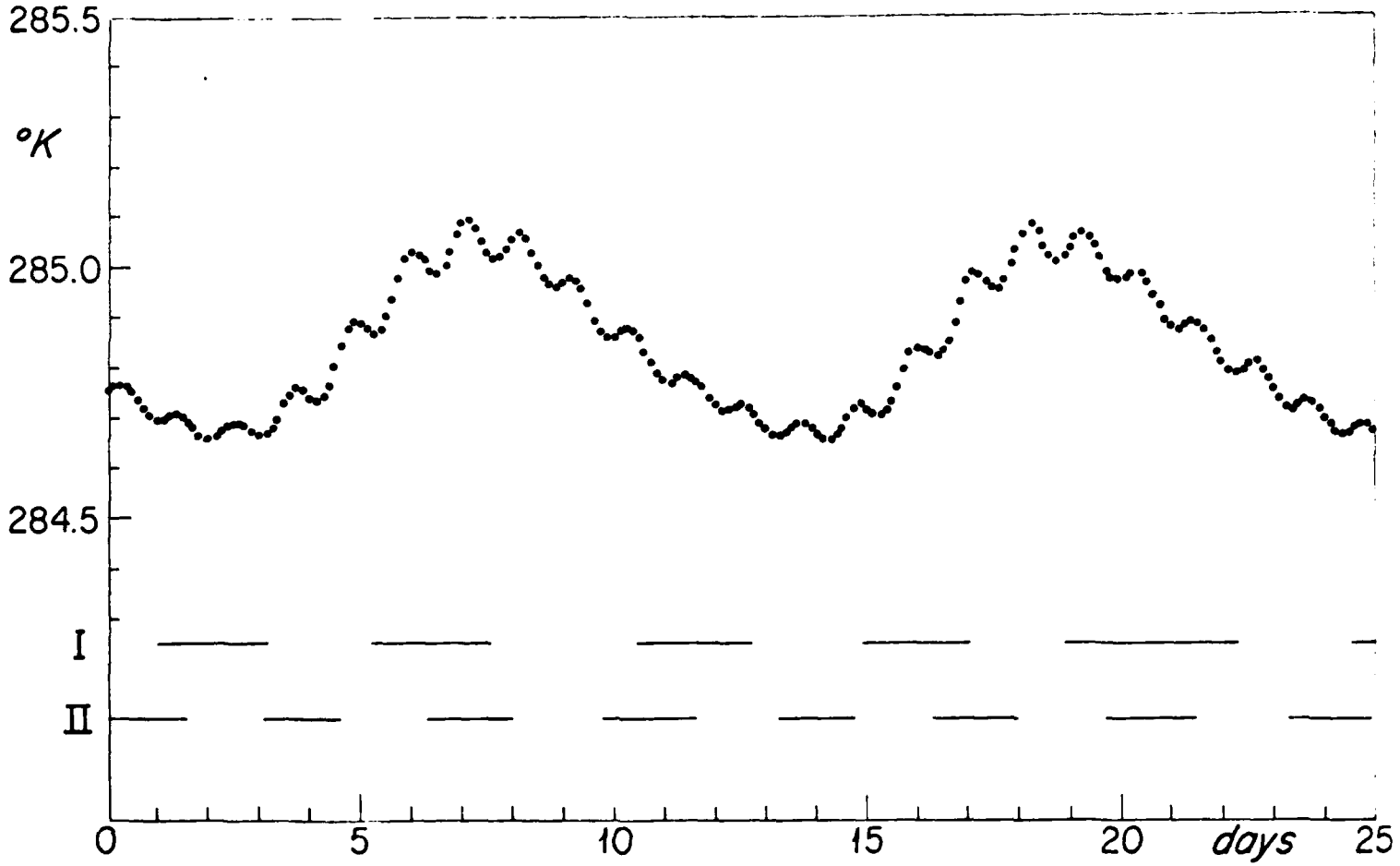

Fig. 2. Instantaneous values of T_0 at 3-hour intervals in Run 2, where $\lambda = 0.175$, $T_0^* = 273.0$, $T_3^* = 15.0$, and $R = 1.0$. Horizontal line segments indicate times when T_1 (I) and T_4 (II) are positive.

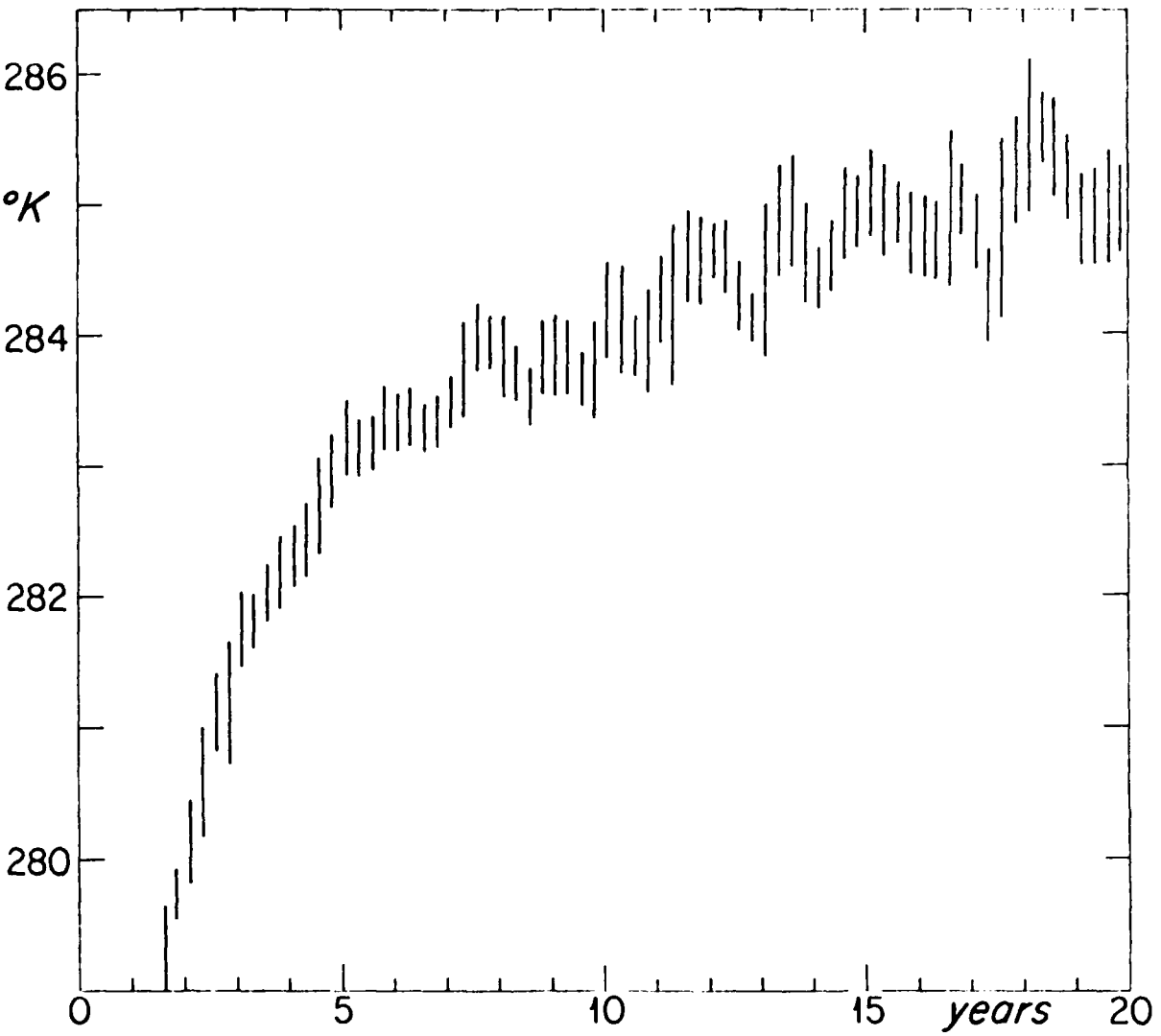

Fig. 3. Ranges of T_0 during consecutive 3-month intervals in Run 4, where $\lambda = 0.2$, $T_0^* = 273.0$, $T_3^* = 10.0$, and $R = 1.0$.

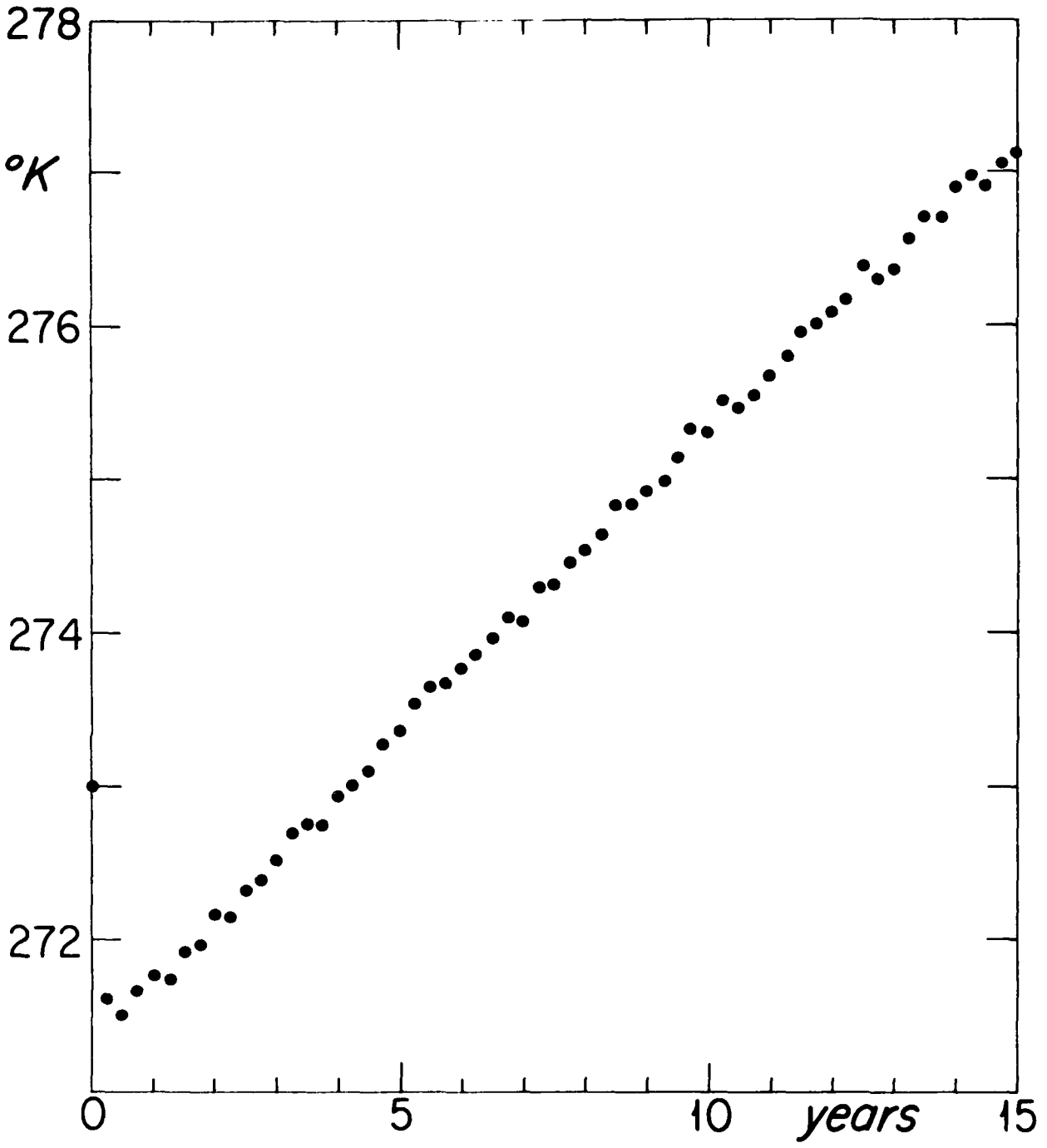

Fig. 4. Instantaneous values of T_0 at 3-month intervals in Run 5, where $\lambda = 0.2$, $T_0^* = 273.0$, $T_3^* = 10.0$, and $R = 25.0$.

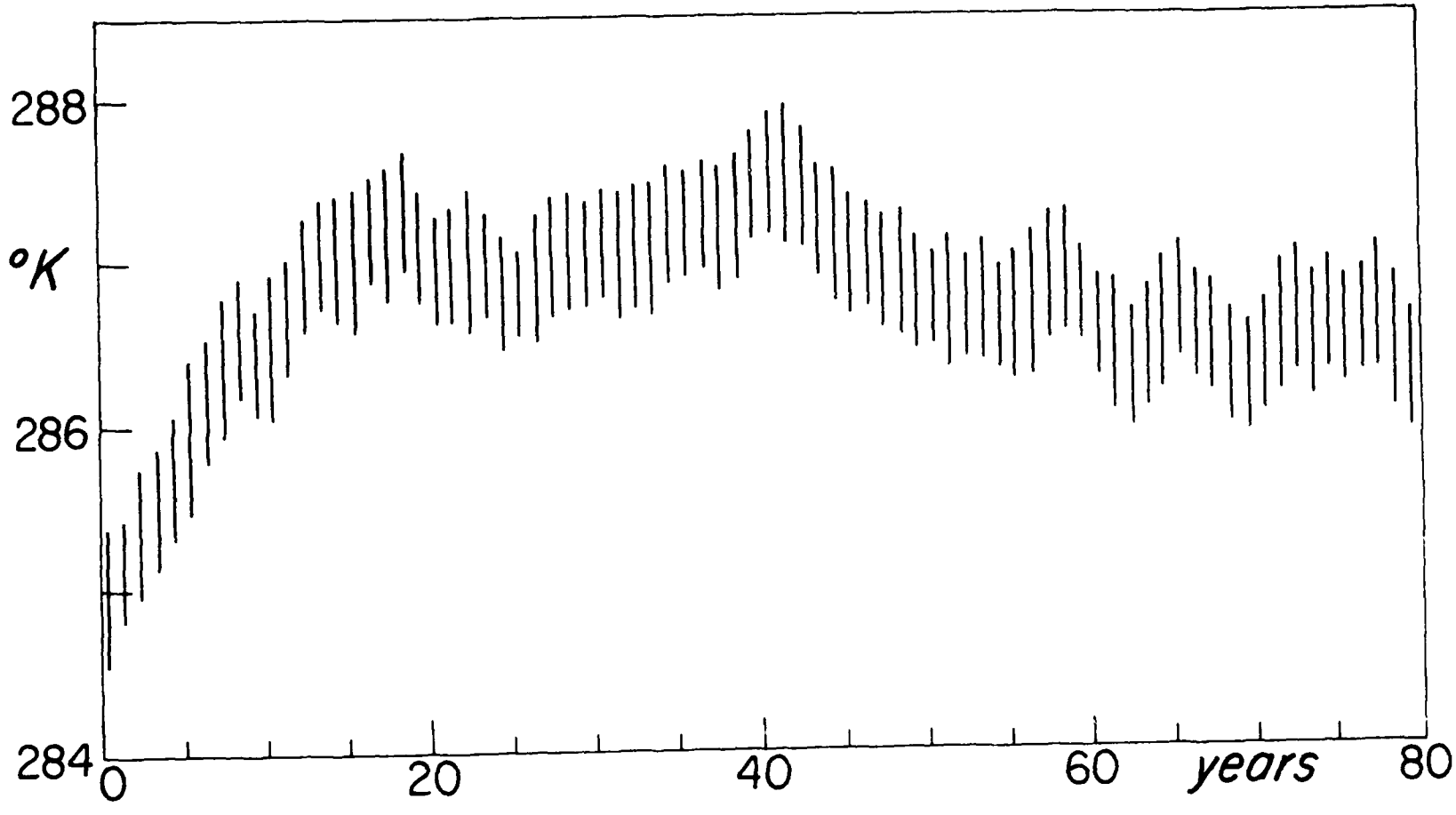

Fig. 5. Ranges of T_0 during consecutive 1-year intervals in Run 6, where $\lambda = 0.2$, $T_0^* = 273.0$, $T_3^* = 10.0$, and $R = 10.0$.

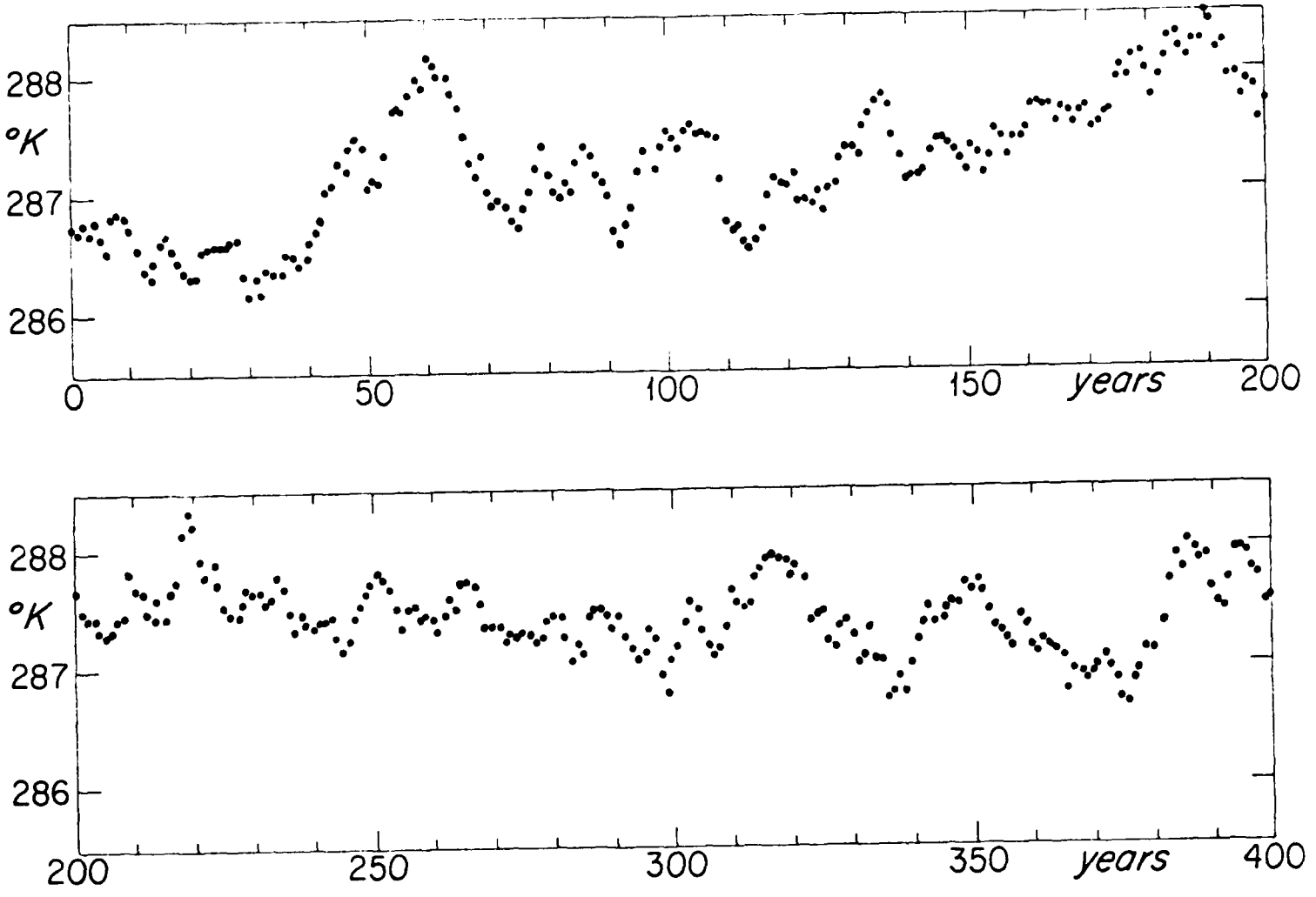

Fig. 6. Consecutive annual average values of T_0 in Run 7, where, as in Run 6, $\lambda = 0.2$, $T_0^* = 273.0$, $T_3^* = 10.0$, and $R = 10.0$.

END

FILMED

12-85

DTIC